

## A NUMERICAL SIMULATION ON THE SOLAR-TERRESTRIAL TRANSIT TIME OF SUCCESSIVE CMES DURING NOVEMBER 4-5, 1998

XIONG Ming ZHENG Hui-Nan WANG Yu-Ming FU Xiang-Rong WANG Shui DOU Xian-Kang

*School of Earth and Space Science, University of Science and Technology of China, Hefei 230026, China*

**Abstract** The solar-terrestrial transit process of three successive coronal mass ejections (CMEs) during November 4~5, 1998 has been investigated numerically in one-dimensional spherical geometry. These CMEs interact with each other while they are propagating in interplanetary space and finally form a “Complex Ejecta”. A Harten’s total variation diminishing (TVD) scheme is applied to solve magnetohydrodynamic (MHD) equations numerically, starting from an ambient solar wind equilibrium, with appropriate dimensionless gravity parameter  $\alpha$ , plasma beta  $\beta$ , and gas polytropic index  $\gamma$ . The equilibrium is consistent in solar wind speed  $v_r$ , proton number density  $N_p$ , and the ratio of proton thermal pressure to magnetic pressure  $\beta_p$  with the observation of ACE spacecraft at Lagrange point ( $L_1$ ). Merely velocity pulse is introduced in the numerical computation, whose amplitude and duration are determined by observation data of Lasco/C2, GOES, LEAR combined with CME’s “Cone Model” proposed by Michalek et al. The results show that the differences of two shock arrival times (SATs) between the numerical calculation and ACE observation are 3 and 4 hours respectively. Therefore the numerical model proposed in this paper can estimate SAT and rough shock intensity formed by successive CMEs evolving in interplanetary space and suggests a potential application in SAT prediction for space weather.

**Key words** Coronal mass ejection, Magnetohydrodynamics, Numerical simulation, Space weather.

### 1 INTRODUCTION

CMEs have been found to be the primary source of transient interplanetary disturbances such as magnetic cloud, ejecta and solar energetic particle and etc.<sup>[1]</sup>. They originate from the solar surface, firstly detected remotely by white-light coronagraphs onboard SOHO/Lasco, propagate and evolve themselves through interplanetary space. When an earth-directed CME is associated with strong southward magnetic field at 1 astronomical unit (AU), which can be observed by an on-site spacecraft, it always results in the commencement of a geomagnetic storm<sup>[2,3]</sup>. Therefore more and more numerical, as well as empirical models, have been developed for space weather to predict the interplanetary parameters variance in the vicinity of Earth orbit.

The conversion from an empirical or semi-empirical predicting model into physics-based one has become a necessity. Among various empirical models, kinetics-based HAF model<sup>[4~7]</sup>, for example, can depict the propagation process of a certain solar eruptive event in interplanetary space and predict disturbance magnitude, interplanetary magnetic field (IMF), plasma density and its bulk flow speed, as well as geomagnetic storm, physical behavior of auroral zone on the basis of satellite observation data. However, numerical prediction models based on MHD equations are the self-consistent mathematical descriptions for space weather phenomenon. MHD models have successfully simulated many important space plasma processes and provided a robust tool for advancing our understanding of such processes. Especially Groth et al.<sup>[8]</sup> applied a parallel adaptive mesh refinement (AMR) finite-volume scheme to MHD simulation and firstly realized global three-dimensional numerical simulation for space weather in demonstrative sense. They gave a simulation example, starting from a CME generated at the solar surface, following by its propagation through interplanetary space and ending in its interaction with the terrestrial magnetosphere-ionosphere system. Groth et al.’s work demonstrates the great potential of a MHD simulation in its application to space weather.

A pivotal step in space weather prediction is to predict SATs incited by solar transients. Gopalswamy et al.<sup>[9,10]</sup> proposed some empirical models to predict the 1AU arrival times of CMEs based on individual CME

events. Gonzalez-Esparza et al.<sup>[11]</sup> applied one-dimensional hydrodynamics numerical model to conduct a parameter study of acceleration and transport time of individual CME events in interplanetary space. However, no studies concerning the complicated interplanetary dynamics behaviors, such as acceleration, deceleration and so on, due to interaction of multi-CMEs in interplanetary space have been involved in the foregoing research<sup>[9~11]</sup>. Burlaga et al.<sup>[12]</sup> studied the successive CME forming complex ejecta from Wind and ACE observation data and found: (1) each component of complex ejecta associates with corresponding CME, but its exact identity is impossible to be scrutinized; (2) initial information nearby Sun as well as each CME characteristic is completely lost during cannibalization process where CME propagation is non-linear and non-retrieval. Meanwhile, there exist some other MHD prediction models, e.g. STOA (The Shock Time of Arrival) based on expansive wave<sup>[13,14]</sup> and ISMP (Interplanetary Shock Propagation Model) model based on 2.5-D MHD model<sup>[14,15]</sup>. However, the results of Riley<sup>[16,17]</sup> and Dryer<sup>[18]</sup> reveal that simplified 1-D numerical model can well reflect the basic physical characteristics of disturbance propagation in interplanetary space. In this paper, aiming at SAT of complex ejecta, we conduct one-dimensional (1-D) MHD numerical simulation to study the propagation and interaction of multi-shocks driven by successive CMEs in spherical geometry. The result shows SAT of complex ejecta formed by Earth-directed fast CMEs could be relatively well estimated through 1-D simulation.

## 2 NUMERICAL SIMULATION ON CME PROPAGATION DURING NOVEMBER 4–5, 1998

### 2.1 MHD Equation Set in Ecliptic Plane

Considering a 1-D MHD in ecliptic plane of spherical coordinate  $(r, \theta, \varphi)$ . All physical quantities depend on the radius  $r$  only, hence magnetic field  $\mathbf{B}$ , bulk flow speed  $\mathbf{v}$ , pressure  $p$  and density  $\rho$  can be expressed as follows:

$$\begin{aligned} B &= B_r(t, r)e_r + B_\varphi(t, r)e_\varphi \\ V &= v_r(t, r)e_r + v_\varphi(t, r)e_\varphi, \\ \rho &= \rho(t, r), \quad p = p(t, r) \end{aligned} \quad (1)$$

The dimensionless MHD equation set is expressed as<sup>[9]</sup>

$$\frac{\partial \mathbf{U}}{\partial t} + \frac{\partial \mathbf{F}}{\partial r} + \mathbf{S} = 0,$$

where

$$\mathbf{U} = \begin{bmatrix} r^2 \rho \\ \rho v_r \\ r^3 \rho v_\varphi \\ r B_\varphi \\ r^2 \left( \rho v_r^2 + \rho v_\varphi^2 + B_\varphi^2 + \frac{\beta p}{\gamma - 1} \right) \end{bmatrix}, \quad (3)$$

$$\mathbf{F} = \begin{bmatrix} r^2 \rho v_r \\ \rho v_r^2 + \frac{\beta}{2} p + \frac{1}{2} B_\varphi^2 \\ r^3 (\rho v_r v_\varphi - B_r B_\varphi) \\ r (B_\varphi v_r - B_r v_\varphi) \\ r^2 \rho v_r \left( v_r^2 + v_\varphi^2 + \frac{\gamma}{\gamma - 1} \frac{\beta p}{\rho} \right) + 2r^2 (B_\varphi^2 v_r - B_\varphi v_\varphi B_r) \end{bmatrix}, \quad (4)$$

$$\mathbf{S} = \begin{bmatrix} 0 \\ \frac{\rho}{r} \left( 2v_r^2 - v_\varphi^2 + \frac{B_\varphi^2}{\rho} + \frac{\alpha}{r} \right) \\ 0 \\ 0 \\ 0 \\ 2\alpha \rho v_r \end{bmatrix}, \quad (5)$$

and

$$B_r = \frac{1}{r^2}. \quad (6)$$

Here  $\rho$ ,  $v$ ,  $B$ ,  $p$ ,  $t$ , and  $r$  are normalized by  $\rho_0$ ,  $V_A$ ,  $B_0$ ,  $p_0$ ,  $\tau_A$ , and  $R_S$  respectively. Moreover,  $\beta = 8\pi p_0/B_0^2$  is the ratio of plasma thermal pressure to magnetic pressure,  $\alpha = gR_S/V_A^2$  is the gravity acceleration dimensionless value,  $\tau_A = R_S/V_A$  and  $V_A = |B_0|/\sqrt{4\pi\rho_0}$  are the characteristic Alfvén time and speed,  $\gamma$  is the gas polytropic index,  $R_S$  is solar radius, and  $g$  is the gravity constant at solar surface.

Among many numerical schemes, Harten's TVD<sup>[20]</sup> has the capability in capturing the shocks sharply and is applied to the MHD numerical computation in this paper. A 1-D MHD numerical model based on the above TVD scheme was established and adopted to solve the related physics.

## 2.2 Initial Equilibrium of 1-D Solar Wind and Input of Disturbance

The equation set of dimensionless form for equilibrium state of 1-D solar wind is

$$v \frac{dv}{dr} + \frac{\beta}{2} \frac{1}{\rho} \frac{dp}{dr} + \frac{\alpha}{r^2} = 0, \quad (7)$$

$$\rho v r^2 = \text{const}, \quad (8)$$

$$p \rho^{-\gamma} = \text{const}, \quad (9)$$

where  $v$  is radial speed. Eq.(8~9) can be reduced to

$$v \frac{dv}{dr} \left[ 1 - \frac{a^2}{v^2} \right] = \left[ \frac{2a^2}{r} - \frac{\alpha}{r^2} \right]. \quad (10)$$

Here  $a^2 = \frac{\beta\gamma p}{2\rho}$ . It can be found that  $v_c^2 = a_c^2 = \frac{\beta\gamma p_c}{2\rho_c}$  at the critical point of acoustic mode,  $r = r_c = \frac{\alpha}{2a_c^2}$ . Solar wind velocity satisfies the following equation

$$\frac{v^2}{a_c^2} + 3 - \frac{4r_c}{r} + \frac{2}{\gamma-1} \left[ \left( \frac{a_c^2 r_c^4}{v^2 r^4} \right)^{\frac{\gamma-1}{2}} - 1 \right] = 0. \quad (11)$$

Thus  $v^2/a_c^2$ , in dependence of  $r/r_c$ , can be solved by iteration method, thereby  $\rho$  and  $p$  are also derived<sup>[21]</sup>. Subscript c denotes the value at critical point. Besides,  $v_\varphi$  and  $B_\varphi$  are all zero in Heliosphere Equator Coordinate (HEQ).

Burlaga et al.<sup>[12]</sup> analyzed the observation data of ACE spacecraft during November 7~10, 1998, and identified "complex ejecta" in interplanetary space and its associated CMEs nearby the solar surface. The first occurrences of these CMEs at Lasco/C2 view field are 04:54UT 11/04/1998, 02:25UT 11/05/1998 and 20:59UT 11/05/1998 respectively. These CMEs are proved to be earth-directed by good symmetry of bright loop of the halo CMEs images in Lasco/C2, Lasco/C3 and evident eruptive activities at solar surface observed by EIT. The simplified 1-D model here can roughly simulate the almost straightforward propagation process of these CMEs in interplanetary space. The projected speed on sky-plane of these three successive halo CMEs are 527km/s, 577km/s, 1124km/s, whose realistic speeds are estimated as 541km/s, 482km/s, 1283km/s by Michalek et al.<sup>[22]</sup> via CME "cone model".

In numerical simulation, proton and electron of solar wind are assumed to have the same temperature, and gas polytropic index  $\gamma = 1.2$ . The scaling parameters in computation are selected from local values at acoustic mode critical point of ambient solar wind, i.e. gravitation acceleration  $\alpha = 6.5$ , the ratio of thermal pressure to magnetic pressure  $\beta = 3.24 \times 10^{-3}$ , solar wind speed 171km/s, proton density  $N_0 = 60464 \text{cm}^{-3}$ , temperature  $T_0 = 1.48 \times 10^6 \text{K}$  and magnetic field  $B_0 = 0.438 \text{Gauss}$ . Initial equilibrium is plotted in Fig.1, where bulk flow speed at solar surface is 58km/s, the ratio of proton thermal to magnetic pressure  $\beta_p = 8.96 \times 10^{-4}$ . The latitude component of magnetic field is ignored since the model deals only within ecliptic plane. It is inevitable

to have smaller quantities for particle density and plasma  $\beta_p$  nearby solar surface while the appropriate physical parameters at Lagrange point  $L_1$  being consistent with satellite observation for 1-D Parker solar wind model. Fig.2 illustrates this event-associated interplanetary CME recorded by ACE at  $L_1$  (about  $213.25R_S$ ), where the two vertical lines denote two shocks “S1” and “S2”. In Fig.2, ACE observation, preceding the shock arrival, illustrates ambient solar wind. It is consistent with initial equilibrium of numerical calculation at  $L_1$ , i.e.  $v_r = 401\text{km/s}$ ,  $\beta_p = 0.47$ ,  $N_p = 6\text{cm}^{-3}$  (explained in Section 2.3 with more detail). Numerical simulation is carried out between  $1R_S$  and  $216R_S$  (about 1AU), in totally 4301 grids with a spacing of  $0.05R_S$ . The simulation, beginning from 04:54UT 11/04/1998, lasts 130 hours.

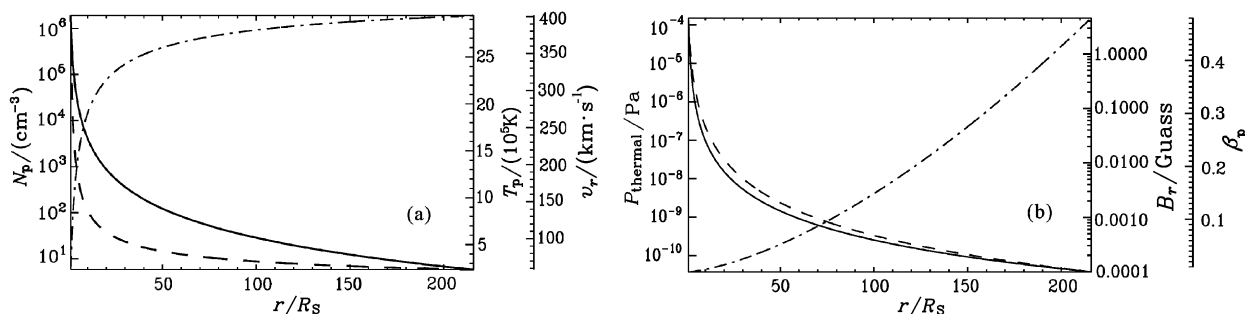


Fig.1 Initial distribution of various physical parameters

Solid, dashed and dot dashed lines at (a) denote proton number density  $N_p$ , proton temperature  $T_p$ , solar wind radial speed  $v_r$ , respectively; those at the (b) denote thermal pressure  $P_{\text{thermal}}$ , radial magnetic field  $B_r$ , the ratio of proton thermal pressure to magnetic field  $\beta_p$ , respectively.

Gopalswamy’s statistical results<sup>[9,10]</sup> showed that the shock arrival time (SAT) at 1AU has weak correlation with internal magnetic structure of CME. Gonzalez-Esparza et al.<sup>[11]</sup> applied a 1-D hydrodynamics numerical model to investigate the typical parameters of acceleration and transport time of individual CMEs through interplanetary space and found that the disturbance magnitude of radial speed is a decisive factor for solar-terrestrial transport time of fast CME. Hence when concerning the transport time of strong disturbance, we merely introduce three velocity pulses at  $3R_S$  (local solar wind speed is  $163\text{km/s}$ ), with commencements at 04:54UT 11/04/1998, 02:25UT 11/05/1998, 20:59UT 11/05/1998 based on LASCO observation. Disturbed local solar wind speeds are estimated by Michalek et al.<sup>[22]</sup>. The durations of CME can be simply estimated by that of associated flare since they are different active phenomena incited by the identical magnetic structure instability. Table 1 is summarized in time, location, active region of CME-associated flares by Burlaga et al.<sup>[12]</sup> and the web site: <http://spidr.ngdc.noaa.gov/spidr/index.html>, where three rows correspond to three successive CME events. From solar surface location of flare occurrence, the same flare event are recorded twice by GOES and LEAR, in regions N17E1 and N19W11 respectively. Thus the durations of the above 3 CMEs are estimated as 48, 20, 72 minutes by simply summing up the duration of independent flare events in each row.

**Table 1 X ray solar flare events accompanied with Earth-directed halo CMEs during 4-5 November 1998**

Category	Date	Observatory	Start (UT)	Peak maximum brightness of X ray flare (UT)	End (UT) at solar surface	Location occurrence	Activity region
1	1998-11-04	GOES	3:10	3:37	3:58	N17E1	8375
	1998-11-04	LEAR	3:14	3:17	4:07	N17E1	8375
2	1998-11-05	LEAR	2:36	2:36	2:49	S29E14	8376
	1998-11-05	GOES	2:57	3:00	3:04	N19W11	8375
	1998-11-05	LEAR	2:59	3:02	3:08	N19W11	8375
3	1998-11-05	GOES	19:00	19:55	20:12	N22W18	

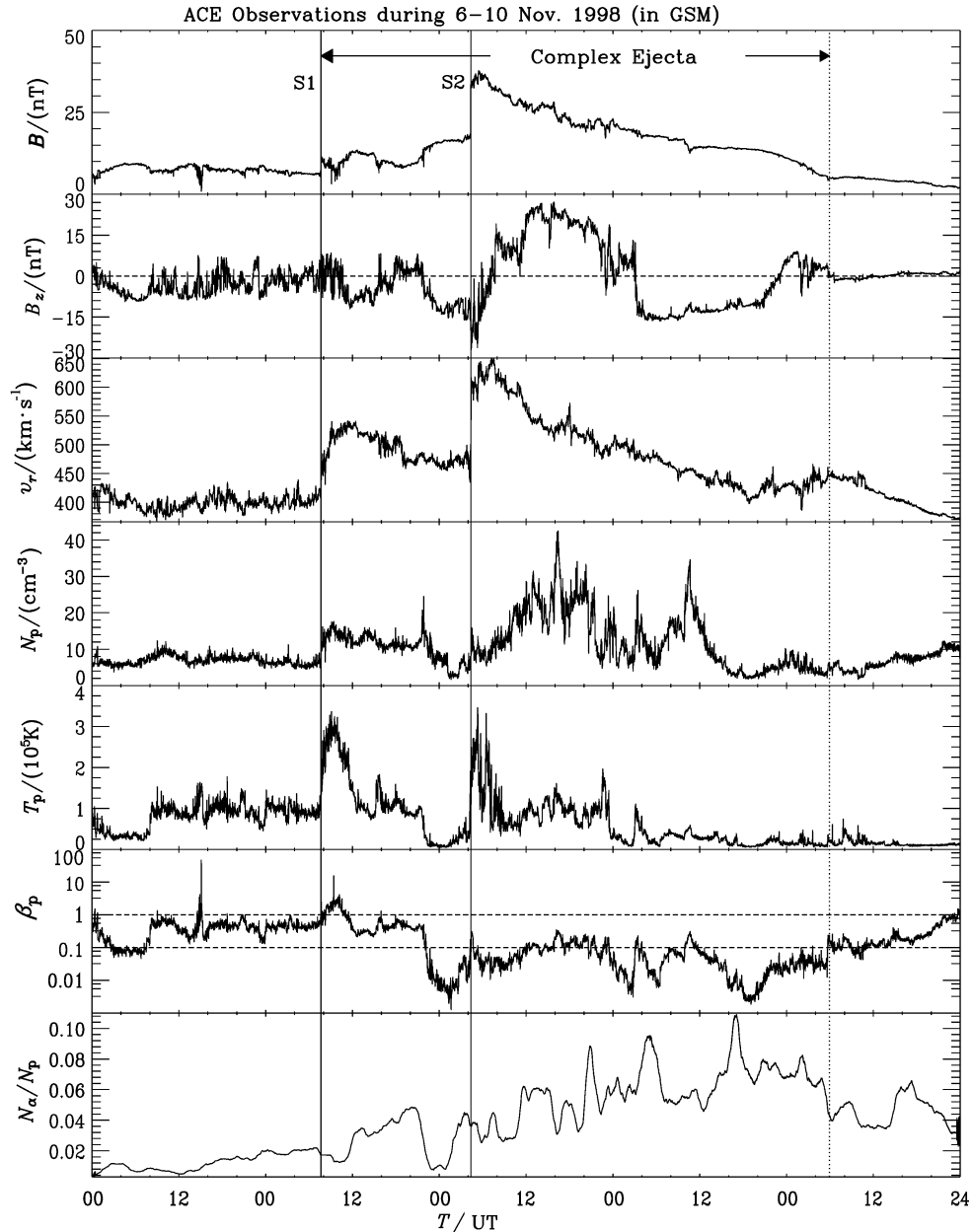


Fig. 2 Observations of solar wind plasma and IMF by ACE spacecraft during November 6~10, 1998.  $B$ ,  $B_z$ ,  $v_r$ ,  $N_p$ ,  $T_p$ ,  $\beta_p$ ,  $N_\alpha/N_p$  are magnetic field strength,  $z$  component field, radial solar wind speed, proton density, proton temperature, the ratio of proton thermal pressure to magnetic pressure and the density ratio of  $He^{++}$  to proton, respectively. Vertical lines denote the times of two successive shocks  $S1$ ,  $S2$  respectively.

### 2.3 Case Studies

Figure 3 exhibits the characteristics of disturbance propagation formed by successive ejecta.  $F$  and  $B$  denote the forward and backward part in a fast mode wave pair. While subscripts 1, 2, 3 represent the three injected disturbances respectively. Disturbance 1 is quickly decomposed into a fast wave pair ( $F_1$  for forward and  $B_1$  for backward) at  $t = 3.95$  hours. The forward fast wave of disturbance 2 ( $F_2$ ) overtakes the backward fast one of disturbance 1 ( $B_1$ ), they mix up at  $t = 42.18$  hours and separate subsequently. At  $t = 62.52$  hours, the forward fast wave of disturbance 3 ( $F_3$ ) penetrates  $B_1$  and approaches the tail of  $F_2$ . Finally  $F_2$  and  $F_3$  merge into a stronger forward fast shock ( $F_2 + F_3$ ). This compound fast shock ( $F_2 + F_3$ ) fails to overtake

$F_1$  in 1AU. It finally results in a two-peak structure observed at Lagrange point  $L_1$ . Fig. 4 displays the time evolution of various physical parameters at Lagrange point  $L_1$ . Initial equilibrium of numerical model has been chosen to ensure a good agreement in physical parameters (Fig. 4) with that of ACE observation (Fig. 2) ahead of shock arrival. One can see that the enhanced  $\beta_p$  from numerical result (Fig. 4) is quite contrary to that from ACE observation (Fig. 2) when the disturbance reaches at  $L_1$ . This is caused by introducing merely velocity disturbance rather than magnetic structure output. Meanwhile all the other parameters  $v_r$ ,  $N_p$  and  $T_p$  in simulation are coincident in morphology with that of observation. The differences of two successive shock arrival times (SATs) between the numerical calculations (11:00UT November 7, 0:00UT November 8 in Fig. 4) and ACE observation (8:00UT November 7, 4:00 UT November 8 in Fig. 2) are 3 and 4 hours respectively.

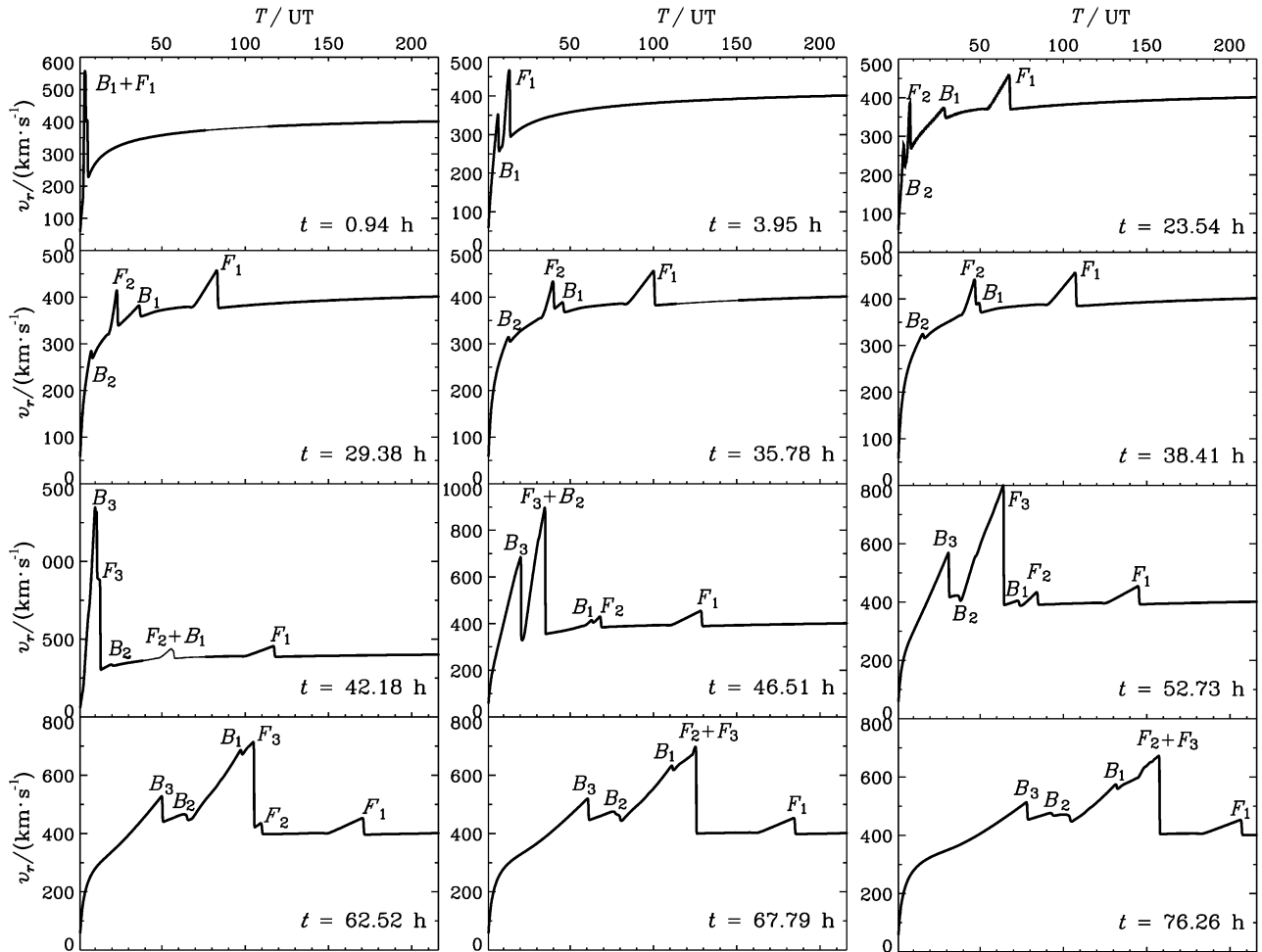


Fig. 3 The time evolution curve of solar wind radial speed incited by disturbance propagation

$F$ ,  $B$  denote forward and backward fast mode wave, subscripts 1,2 and 3 denote three wave modes related with injected three disturbances respectively.

In order to accentuate the influence of interaction among CMEs through interplanetary space upon SAT, numerical calculation has also been carried out for the three disturbances of this complex ejecta separately. The results are shown in Fig. 5. (1) Each shock propagates through interplanetary space at approximately identical speed, in consistent with Vandas's conclusion<sup>[23]</sup> that magnetic cloud finally propagates at asymptotic speed in interplanetary ecliptic plane. (2) The difference of calculation in compound event from that in separate events is that the fronts of disturbances 2 and 3 merge into a compound shock front when they collide in interplanetary space. Therefore disturbances 2 and 3, though beginning at different time, arrive at  $L_1$  simultaneously, which

advances SAT of disturbance 2 by 10 hours or so (as seen in Fig. 6). This indicates that Gopalswamy’s empirical formula based on statistical result of individual CME events could not be applied to the interaction process of multi-CMEs among complex ejecta. Our results show that the proposed 1-D numerical model can estimate SAT and rough shock intensity formed by successive Earth-directed fast CMEs evolving in interplanetary space.

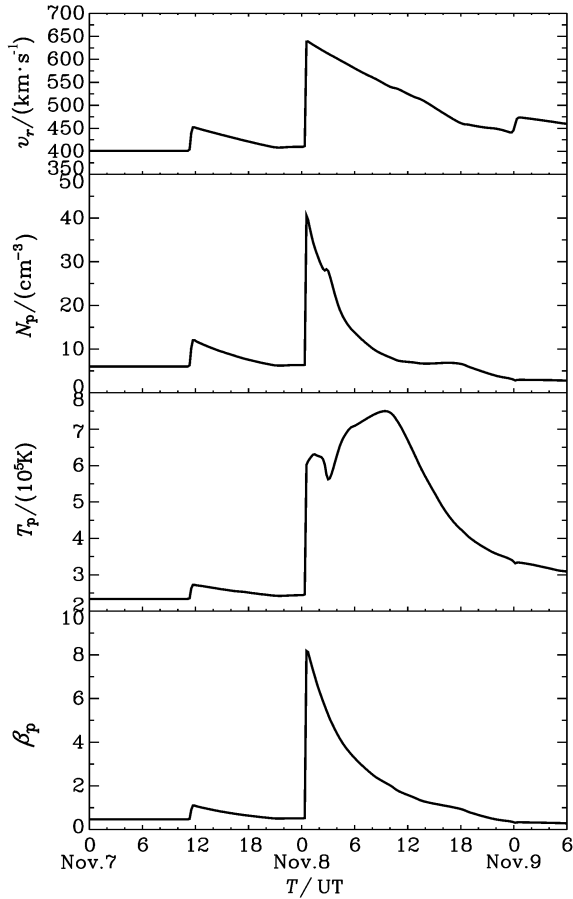


Fig. 4 The time evolution curves of  $v_r$ ,  $N_p$ ,  $T_p$  and  $\beta_p$  at Lagrange point  $L_1$  obtained from numerical simulation

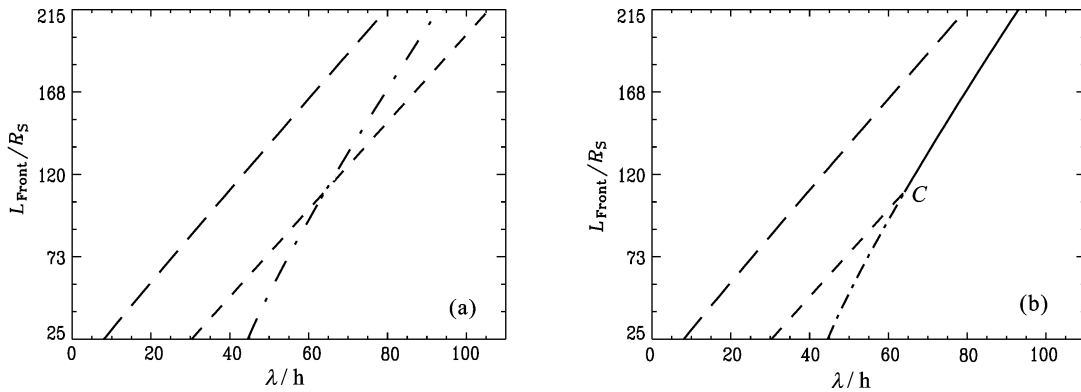


Fig. 5 The location-time ( $L_{Front}-\lambda$ ) relationship of shock front in interplanetary space  
 (a) Separate ejecta; (b) Complex ejecta. Long dashed, dashed, dot dashed and solid lines denote the wave front of disturbances 1, 2, 3, and compound front due to collision at point “C” respectively.

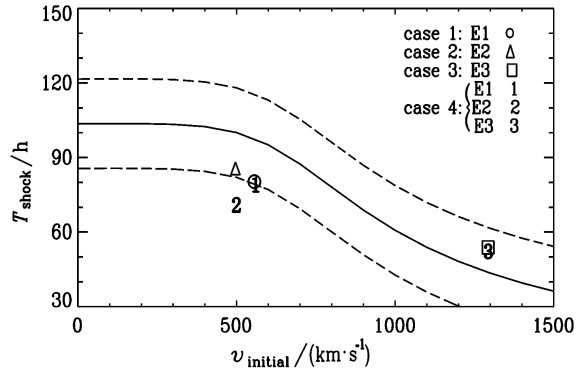


Fig. 6 The relationship of shock transport time

$T_{shock}$  and CME initial speed  $v_{initial}$

E denotes ejecta.  $T_{shock}$  refers to the time difference between shock arrival at Lagrange point ( $L_1$ ) and its corresponding CME firstly observed by Lasco/C2. Solid line and dashed line denote Gopalswamy’s empirical formula and its error band<sup>[10]</sup>. Cases 1, 2, 3 denote hypothetical separate ejecta, denoted by  $\circ$ ,  $\Delta$ ,  $\square$  respectively. Case 4 denotes complex ejecta and 1, 2, 3 denote corresponding three successive CMEs. Note: disturbances 2 and 3, though starting at different times, arrive at point  $L_1$  simultaneously.

### 3 CONCLUSIONS

The evolution process of the three successive CMEs during November 4-5, 1998 has been investigated numerically in ecliptic plane with 1-D spherical coordinates. The results indicate that the numerical model in this paper can estimate SAT and rough shock intensity formed by fast CME via merely introducing velocity pulse. Moreover, MHD numerical simulation can demonstrate the propagation and evolution of the disturbance. It can also describe the propagation characteristic of individual waves as well as interaction among multi waves in interplanetary space. Therefore the proposed numerical model is more feasible than Gopalswamy's empirical formula base on individual events<sup>[9,10]</sup> and suggests a potential application in SAT predication for space weather.

### ACKNOWLEDGEMENT

This work was supported by the National Natural Science Foundation of China (40274050, 40336052, 40404014), the Ministry of Science and Technology of China (NKBRF G2000078405) and the Chinese Academy of Sciences (KZCX2-SW-136). The authors also acknowledge the use of observation data from SOHO, ACE, GOES spacecrafts and LEAR observatory with gratitude.

### REFERENCES

- [1] Gosling J T. The solar flare myth. *J. Geophys. Res.*, 1993, **98(A11)**: 18,937~18,950
- [2] Akasofu S I. Energy coupling between the solar wind and the magnetosphere. *Space Sci. Rev.*, 1981, **28**: 121~190
- [3] Gonzalez W D, Gonzalez L C, Tsurutani B T, et al. Solar wind-magnetosphere coupling during intense magnetic storms (1978~1979). *J. Geophys. Res.*, 1989, **94**: 8,835~8,851
- [4] Hakamada K and Akasofu S I. Simulation of three-dimensional solar wind disturbances and resulting geomagnetic storms. *Space Sci. Rev.*, 1982, **31**: 3~70
- [5] Akasofu S I, Fry C D. A first-generation geomagnetic storm prediction scheme. *Planetary Space Sci.*, 1986, **34**: 77~92
- [6] Fry C D, Sun W, Deehr C S, et al. Improvements to the HAF solar wind model for space weather predictions. *J. Geophys. Res.*, 2001, **106(A10)**: 20985~21001
- [7] Wang C B, Zhao J K, Chen H H, et al. Prediction of the IMF  $B_z$  using a 3-D kinematic code. *Chinese J. Geophys.*, (in Chinese), 2002, **45(6)**: 749~758
- [8] Groth C P T, De Zeeuw D L, Gombosi T I, et al. Global 3D MHD simulation of a space weather event: CME formation, interplanetary propagation, and interaction with the magnetosphere. *J. Geophys. Res.*, 2000, **105(A11)**: 25,053~25,078
- [9] Gopalswamy N, Lara A, Lepping R P, et al. Interplanetary acceleration of coronal mass ejections. *Geophys. Res. Lett.*, 2000, **27**: 145~148
- [10] Gopalswamy N, Lara A, Yashiro S, et al. Predicting the 1-AU arrival times of coronal mass ejections. *J. Geophys. Res.*, 2001, **106(A12)**: 29207~29218
- [11] Gonzalez-Esparza J A, Lara A, Perez-Tijerina E, et al. A numerical study on the acceleration and transit time of coronal mass ejections in the interplanetary medium. *J. Geophys. Res.*, 2003, **108(A1)**: SSH9
- [12] Burlaga L F, Plunkett S P, st Cyr O C. Successive CMEs and complex ejecta. *J. Geophys. Res.*, 2002, **107(A10)**: SSH1
- [13] Smart D F, Shea M A. A simplified model for timing the arrival of solar-flare-initiated shocks. *J. Geophys. Res.*, 1985, **90**: 183~190
- [14] Smith Z, Dryer M, Ort E, et al. Performance of interplanetary shock prediction models: STOA and ISPM. *J. Atmos. Solar-Terr. Phys.*, 2000, **62**: 1265~1274
- [15] Smith Z, Dryer M. MHD study of temporal and spatial evolution of simulated interplanetary shocks in the ecliptic plane within 1 AU. *Solar Phys.*, 1990, **129**: 387~405
- [16] Riley P, Gosling J T. Do coronal mass ejections implode in the solar wind? *Geophys. Res. Lett.*, 1998, **25**: 1529~1532
- [17] Riley P, Gosling J T, Pizzo V J. Investigation of the polytropic relationship between density and temperature within interplanetary coronal mass ejection using numerical simulations. *J. Geophys. Res.*, 2001, **106(A5)**: 8291~8300

- [18] Dryer M. Interplanetary studies: Propagation of disturbances between the Sun and the magnetosphere. *Space Sci. Rev.*, 1994, **67**: 363~419
- [19] Jeffrey A, Taniuti T. Non-linear wave propagation with applications to physics and magnetohydrodynamics. New York: Academic Press, 1964
- [20] Harten A. High resolution schemes for hyperbolic conservation laws. *J. Comput. Phys.*, 1983, **49**: 357~393
- [21] Parker E N. Interplanetary dynamical processes. New York: Wiley-Interscience, 1963
- [22] Michalek G, Gopalswamy N, Yashiro S. A new method for estimating widths, velocities and source location of halo CMEs. *Astrophys. J.*, 2003, **584**: 472~478
- [23] Vandas M, Fischer S, Dryer M, et al. Simulation of magnetic cloud propagation in the inner heliosphere in two-deimensions 1. A loop perpendicular to the ecliptic plane. *J. Geophys. Res.*, 1995, **100(A7)**: 12,285~12,292